

## STRUCTURE OF CHALCOGENIDE GLASSES IN As-S-Se SYSTEM INVESTIGATED BY RAMAN SPECTROSCOPY AND FIRST PRINCIPLE CALCULATION

X. HAN, H. TAO<sup>\*</sup>, L. GONG<sup>a</sup>, J. HAN, S. GU

*State key laboratory of silicate materials for architectures (Wuhan University of Technology), Wuhan, 430070, P.R. China*

*<sup>a</sup>Faculty of Materials, Optoelectronics and Physics, Xiangtan University, Xiangtan, Hunan 411105, PR China*

We report an investigation of Raman spectroscopy on the structure of  $\text{As}_{40}\text{S}_x\text{Se}_{60-x}$  glasses prepared by conventional melt-quenching techniques with As, S and Se of 99.99% purity. And vibrational modes of  $\text{AsS}_n\text{Se}_{3-n}$  clusters were calculated by Gaussian software based on Density functional theory (DFT). It can be found that the calculated data of basic cluster models are in excellent agreement with observed Raman spectra and we found the frequency variation of main vibrational modes for four basic  $\text{AsS}_x\text{Se}_{3-x}$  pyramids can be explained by force constant and reduced mass, according to the molecular spectroscopy theory. Finally, the shift of main Raman scattering frequency of structural units of  $\text{AsS}_n\text{Se}_{3-n}$  pyramids in the Raman spectroscopy of  $\text{As}_{40}\text{S}_x\text{Se}_{60-x}$  glasses can be attributed to the alteration of the nearest neighbor local surroundings with different ratios of S/Se.

(Received February 24, 2014; Accepted April 8, 2014)

*Keywords:* As-S-Se glass; Raman scattering; ab initio calculation.

### 1. Introduction

Chalcogenide glasses and their function in a wide range of optical, electronic and memory applications, have proved a very fertile field of experimental and theoretical research over the past 30 years[1]. As a result of several applications of these materials, those glasses are the outcome of an influencing variety of athermal photoinduced phenomena. Among the most promising applications of chalcogenide glasses, a large majority of studies have concentrated on the stoichiometric  $\text{As}_2\text{S}_3$  due to its excellent stability. However, ternary chalcogenide glasses especially for As-S-Se system are of much interest as the addition of selenium permits to tune and widen the optical transparency and to improve the non-linear properties[2]. Therefore, the focus of recent research related to mixed S-Se glasses are reported to investigate the mechanism of photostructural changes and to inspect the relative contribution of S and Se to the photosensitivity especially with different S/Se composition[3]. Meanwhile, Thin films of  $\text{As}_2\text{S}_3$  and  $\text{As}_2\text{Se}_3$  were deposited and characterized by scanning electron microscopy (SEM), X-ray diffraction and optical absorption techniques[4]. Despite the development of experimental technology, the underlying structure in As-S-Se glass and electronic phenomena taking place during photo-induced processes are still not well understood. In addition, no one model has been able to explain all modifications that happen in As-S-Se glass. Unlike for crystalline system-ray and neutron diffraction applied to glass can only provide a partial characterization of the atomic structure because of the lack of long-range order. In recent year, first-principle approaches have also addressed dynamical properties making contact with vibrational spectroscopies, such as inelastic neutron scattering,

---

\* Corresponding author: thz@whut.edu.cn

infrared absorption, and Raman scattering, which are considered as effective analysis tools to account for microstructure of amorphous system [5]. At present, there are several methods of investigation, which have been used to acquire insight into the structural properties of chalcogenide glassy systems such as ab initio method of Hartree-Fock theory [1, 6], density functional theory (DFT)[7] and method of analogy between clusters, which have similar microstructure and reduced mass[8].

Although chalcogenide materials, including chalcogenide glasses have been extensively studied many years and most of the data published to date has concentrated on amorphous Se, amorphous or crystalline  $\text{As}_2\text{S}_3$  and  $\text{As}_2\text{Se}_3$ , to our knowledge, few studies were focusing on the change of microstructure in As-S-Se glass with different S/Se ratio. In this paper, the structural transformation of ternary As-S-Se chalcogenide system was investigated with Raman spectroscopy and models of basic structure of As-S-Se glasses were calculated using Density functional theory (DFT) by Gaussian software. Therefore, the present investigation is focused on the structural feature and vibrational properties of  $\text{As}_{40}\text{S}_x\text{Se}_{60-x}$ , ( $0 < x < 60$ ) and Raman scattering provides unique capability for a detailed description of the glass structure due to the species-specific nature of vibrational modes. Furthermore, to interpret the experimental data from Raman spectroscopy, we also present main vibrational mode of many basic models of As-S-Se glass system based on the Density functional theory.

## 2. Material and methods

### 2.1 Experimental details

The source materials of the chalcogenide glasses were prepared by synthesizing  $\text{As}_{40}\text{S}_x\text{Se}_{60-x}$  with different alloy compositions of  $x=0,15,30,45,60$ . appropriate amount of arsenic, selenium and sulfur with 99.999% purity were put into fused quartz ampoules which were put in evacuated (Vacuum: 10-1 Pa) and then inserted into a rocking furnace. The batches were held at  $700\sim 750^\circ\text{C}$  for 8~24 hours in order to assist the reaction among As, S and Se and subsequently the temperature was lowered to  $600^\circ\text{C}$ . With a view to stabilizing the melts for homogeneity without rotation, we keep placing for 1 hour with close of the rock and these samples were quenched in water at a temperature of  $\sim 15^\circ\text{C}$  for a few seconds. Raman spectra were obtained by a Fourier transform Raman spectrometer. For the avoidance of local laser damage, an Ar laser ( $\lambda=514.5\text{nm}$ ) with a power less than 20mV was used as an excitation source and the resolution in the frequencies was  $\pm 2\text{cm}^{-1}$ .

### 2.2 Theoretical and calculation details

In the year of 1972, G.Lucovsky[9] demonstrate a molecular model to calculate optic mode frequencies in chalcogenide glass. They considered there two types of vibrations exist in  $\text{As}_2\text{X}_3$  ( $\text{X}=\text{S}, \text{Se}, \text{Te}$ ) glass system. One was vibrational modes in pyramid  $\text{AsX}_3$ ; the other was the vibration mode of As-X-As bent chain, which generates the interaction between the  $\text{AsX}_3$  pyramid molecules. For the  $\text{As}_2\text{S}_3$  and  $\text{As}_2\text{Se}_3$  glass systems, however, the inter-molecular coupling is so weak that vibrational modes of molecule ( $\text{AsX}_3$ ) and bridging chain (As-X-As) can be treated independently. In addition, Wanyan Li et al[10] consider there are four possible  $\text{AsS}_{3-n}\text{Se}_n$  pyramids ( $n=0,1,2,3$ ) and three pyramids with  $\text{AsS}_2\text{Se}$ ,  $\text{AsSSe}_2$  and  $\text{AsSe}_3$  can contribute to As-Se vibration. Based on the molecular model above, all calculations reported in this paper were performed with the Gaussian program package based on density functional theory in order to calculate the basic structural details and vibrational frequencies of four possible molecular units  $\text{AsS}_n\text{Se}_{3-n}$  ( $n=0, 1, 2, 3$ ). To study the Raman-active modes of  $\text{AsS}_n\text{Se}_{3-n}$ , however, we use finite clusters of atoms containing structural units [7], which are considered to be significant in glasses. Dangling bonds on the cluster surfaces are terminated by H atoms in order to construct the neutral chemical environment and because of the large mass difference between H and the heavy atoms related to As, S and Se preventing H atom motion from mixing strongly in the As-S and As-Se vibrational modes, the H atom-related modes lie well outside the spectral region of interest for  $\text{AsS}_x\text{Se}_{3-x}$  and any H atom modes can be easily removed from the analysis of the region with As-S and As-Se vibrational modes. In addition, the method of adding terminal H atoms is widely used in the cluster calculation research [1, 6]. The geometrical optimizations of all the basic structures

under the ground state were at the B3LYP/3-21G level, which was widely used to calculate other molecules[11]and exhibited successful results of vibration mode frequencies in  $AsS_nSe_{3-n}$  ( $n=0, 1, 2, 3$ )clusters, compared with the experimental data from Raman spectra.

### 3. Results

Table 1 shows the optimized geometries about bond distances and angles for the clusters of  $AsS_nSe_{3-n}$  ( $n=0, 1, 2, 3$ ).It can be seen that the calculated bond distance and angle is similar to those of experimental data, which indicates the optimized structure are reasonable to stand for the real clusters in  $AsS_3(AsSe_3)$  glass systems. In addition, we can realize the bond distance of As-S increase from 2.387Å, 2.397Å to 2.404Åwith the increasing Se atoms in clusters of  $AsS_nSe_{3-n}$ , which resemble that of As-Se increase from 2.505Å, 2.512Å to 2.520Å.

Table 1. Calculated bond distance and angle and observed bond distance in  $AsS_nSe_{3-n}(n=0,1,2,3)$

Model	$AsS_3$	$AsS_2Se$	$AsSSe_2$	$AsSe_3$
Calculated bond distance(Å)				
r(As-S)	2.387	2.397	2.404	----
r(As-Se)	----	2.505	2.512	2.520
Observed bond distance(Å)[10]				
r(As-S)	2.32			
r(As-Se)				2.49
Calculated bond angles (degrees)				
S-As-S	95.7	94.4	----	----
S-As-Se	----	103.4	92.2	----
Se-As-Se	----	----	90.3	95.5
Observed bond angles (degrees)[12,13]				
S-As-S	~98			
Se-As-Se				~95

Table 2 shows all basic vibrational modes of  $AsS_nSe_{3-n}$  ( $n=0, 1, 2, 3$ ) structural units classified by molecular point group [14]. There are four basic vibrational modes in  $[AsS_3]$  and  $[AsSe_3]$  with the point group of  $C_{3v}$ . When it comes to  $[AsSSe_2]$  or  $[AsS_2Se]$ , the number of basic vibrational modes transforms from four to six. In addition, for the molecule of  $XY_3$ ,  $\nu_1$ -type mode stand for the symmetrical stretching vibration and  $\nu_3$ -type mode is attributed to anti-symmetric stretching vibration.

Table 2 Vibrational frequencies of  $AsS_nSe_{3-n}(n=0,1,2,3)$  pyramical cluster calculated at DFT/3-21G level. The first row shows DFT fully optimized ball-and-stick draws of the pyramidal units. Purple:As;Green:S;Red:Se.

$C_{3v}$	$\nu_1(A_1)$	$\nu_2(A_1)$	$\nu_3(E)$	$\nu_4(E)$		
$XY_3$	$\nu_A(XY)$	$\delta_d(YXY)$	$\nu_d(XY)$	$\delta_d(YXY)$		
$AsS_3$	342	133	335	95		
$AsSe_3$	235	94	248	71		
$C_s$	$\nu_1(A')$	$\nu_3(A')$	$\nu_2(A')$	$\nu_5(A'')$	$\nu_4(A')$	$\nu_6(A'')$
$ZXY_2$	$\nu(XZ)$	$\delta_s(YXZ)$	$\nu_s(XY)$	$\nu_a(XY)$	$\delta(YXY)$	$\delta_a(YXZ)$
$AsS_2Se$	258	118	327	329	150	96
$AsSSe_2$	331	109	242	254	137	91

#### 4. Discussion

Table 3 shows the comparison of stretching vibration mode between  $\text{AsCl}_3$  ( $\text{AsBr}_3$ ) and  $\text{AsS}_3$  ( $\text{AsSe}_3$ ) pyramid units. The experimental vibrational mode data of  $\text{AsCl}_3$  and  $\text{AsBr}_3$  comes from the reference [14]. Meanwhile, the calculated vibrational mode data of  $\text{AsS}_3$  and  $\text{AsSe}_3$  is collected from table 2. There is an interesting phenomenon that  $V_s(\text{AsCl}_3)/V_s(\text{AsS}_3)=1.219$  and  $V_s(\text{AsBr}_3)/V_s(\text{AsSe}_3)=1.229$ . Similarly,  $V_{as}(\text{AsCl}_3)/V_{as}(\text{AsS}_3)=1.167$  and  $V_{as}(\text{AsBr}_3)/V_{as}(\text{AsSe}_3)=1.145$ , which indicates there are similar vibrational modes between  $\text{AsCl}_3$  ( $\text{AsBr}_3$ ) and  $\text{AsS}_3$  ( $\text{AsSe}_3$ ) pyramid units, because  $V_s(\text{AsCl}_3)/V_s(\text{AsS}_3)\approx V_s(\text{AsBr}_3)/V_s(\text{AsSe}_3)$  and  $V_{as}(\text{AsCl}_3)/V_{as}(\text{AsS}_3)\approx V_{as}(\text{AsBr}_3)/V_{as}(\text{AsSe}_3)$ . This phenomenon can be explained by the similar mass ratios ( $m_{\text{As}}/m_{\text{S}(\text{Se})}\approx m_{\text{As}}/m_{\text{S}(\text{Se})}$ ) and force constant ratios reported by G. Lucovsky [8].

Table 3. the comparison of stretching vibration mode between  $\text{AsCl}_3$  ( $\text{AsBr}_3$ ) and  $\text{AsS}_3$  ( $\text{AsSe}_3$ ) pyramid units

AsCl3[14]		AsBr3[14]	
$V_s$	$V_{as}$	$V_s$	$V_{as}$
417	391	289	284
AsS3		AsSe3	
$V_s$	$V_{as}$	$V_s$	$V_{as}$
342	335	235	248
AsCl3/AsS3		AsBr3/AsSe3	
1.219	1.167	1.229	1.145

It can be seen from Table 4 that the calculated vibrational mode data of  $\text{AsS}_n\text{Se}_{3-n}$  pyramid clusters are in agreement with the experimental data in the reference [10].

Table 4. The main Raman vibrational frequencies ( $\text{cm}^{-1}$ ) of  $\text{AsS}_n\text{Se}_{3-n}$  clusters

Molecular type	Experimental[10]	Calculated	Main vibrational mode
$\text{AsSe}_3$	227	235	$\nu_1(A_1)$
$\text{AsSSe}_2$	241	242	$\nu_2(A')$
$\text{AsS}_2\text{Se}$	257	258	$\nu_1(A')$
$\text{AsS}_3$	340	342	$\nu_1(A_1)$

The main vibrational modes of four basic pyramid clusters of  $[\text{AsS}_3]$ ,  $[\text{AsS}_2\text{Se}]$ ,  $[\text{AsSSe}_2]$  and  $[\text{AsSe}_3]$  are  $340\text{cm}^{-1}$ ,  $257\text{cm}^{-1}$ ,  $241\text{cm}^{-1}$  and  $227\text{cm}^{-1}$ , which indicates the frequency variation from fast to slow. According to analysis of vibration mode, we can classify all four main vibration modes into two types. One is the stretching vibrational mode related to As-S attributed to  $\text{AsS}_3$ , the other is the stretching vibrational mode related to As-Se belong to  $\text{AsS}_2\text{Se}$ ,  $\text{AsSSe}_2$  and  $\text{AsSe}_3$ . And the vibrational frequency from  $340\text{cm}^{-1}$  to  $257\text{cm}^{-1}$  indicates the vibrational modes from As-S related to As-Se related, so the frequency decreases sharply. Compared to this sharp shift, the difference between  $[\text{AsS}_2\text{Se}]$  and  $[\text{AsSSe}_2]$  is only about  $16\text{cm}^{-1}$ , which is similar to the difference between  $[\text{AsSSe}_2]$  and  $[\text{AsSe}_3]$ . This is because the main vibrational mode all belong to As-Se related for  $[\text{AsS}_2\text{Se}]$ ,  $[\text{AsSSe}_2]$  and  $[\text{AsSe}_3]$ . On the other hand, according to the molecular spectroscopy theory as follows:

$$\nu \propto \sqrt{\frac{f}{\mu}}$$

where  $f$  is a constant related to the bond strength, and  $\mu$  is the discount mass. The vibrational mode from  $[\text{AsS}_3]$  to  $[\text{AsS}_2\text{Se}]$ , the bond of As-S is stronger than that of Se and the atomic mass of Se is heavier than that of S, which indicates force constant of As-S is bigger than that of As-Se. Furthermore, with increasing Se in the pyramids, the mode mass would be somewhat bigger, so the frequency variation shifts sharply. However, when the vibrational modes change from  $[\text{AsS}_2\text{Se}]$ ,  $[\text{AsSSe}_2]$  to  $[\text{AsSe}_3]$  the main vibrational modes all related to As-Se, so the force constants for  $[\text{AsS}_2\text{Se}]$ ,  $[\text{AsSSe}_2]$  and  $[\text{AsSe}_3]$  are more closer to each other than that of As-S related for  $[\text{AsS}_3]$ , which lead to a slow decrease of frequency.

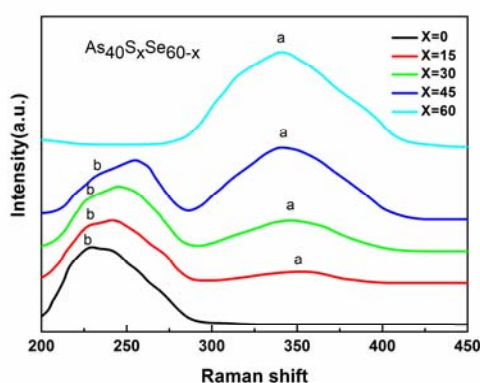


Fig.1. Raman spectra of the  $As_{40}S_xSe_{60-x}$  glasses with  $X=0, 15, 30, 45$  and  $60$

Fig. 1 shows the Raman spectroscopy of  $As_{40}S_xSe_{60-x}$  glasses, which can be classified into two main regions located at  $200\sim 300$  and  $300\sim 400\text{cm}^{-1}$  of stretching vibrational mode related to As-Se and As-S, respectively. According to Research on Raman spectra of  $As_xS_{100-x}$  glasses by R.M.Holomb[15], the broad Raman band of g- $As_2S_3$  consists of at least three individual peaks around  $306, 340$  and  $385\text{cm}^{-1}$ . Meanwhile, the Raman spectrum of polycrystalline  $As_2S_3$  has strong peaks in the area at  $292, 310, 355$  and  $382\text{cm}^{-1}$ . According to Wagner et al [16]. The two shoulders around  $312$  and  $380\text{cm}^{-1}$  of g- $As_2S_3$  Raman spectra are due to interactions among the  $AsS_3$  pyramids. Based on the molecular model by G.Lucovsky[9], the inter-molecular coupling is so weak in the  $As_2S_3$  and  $As_2Se_3$  glass systems, which indicates the Raman vibrational modes related to interactions among  $As_2S_3$  ( $As_2Se_3$ ) are much weaker than those related to intra- $As_2S_3$  ( $As_2Se_3$ ) pyramids. In addition, the peak of  $340\text{cm}^{-1}$  in g- $As_2S_3$  is attributed to the  $\nu_1$  mode of  $AsS_3$  pyramid. Meanwhile, there are two obvious shoulders located at  $\sim 230$  and  $\sim 248\text{cm}^{-1}$  in Raman spectra of g- $As_2Se_3$ , which can be attributed to the symmetrical and asymmetrical vibrational modes of  $AsSe_3$  pyramid. Also, in the As-Se related peak range of  $As_{40}S_xSe_{60-x}$  glasses, the main Raman bands are attributed to the As-Se vibration of  $[AsS_2Se]$ ,  $[AsSSe_2]$  and  $[AsSe_3]$  pyramids ( $230, 241, 257\text{cm}^{-1}$ ) with the vibrational mode of  $\nu_1(A')$ ,  $\nu_2(A')$  and  $\nu_1(A_1)$ , respectively.

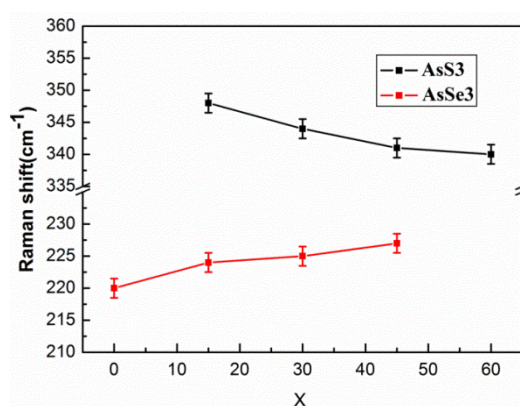


Fig.2. Positions of main Raman vibrational mode of  $AsS_3$  and  $AsSe_3$  pyramidal cluster in the Raman spectra of the  $As_{40}S_xSe_{60-x}$  glass.

From the experimental Raman spectra of  $As_{40}S_xSe_{60-x}$  glass in Fig.1, we can observe the two strong peaks labeled a and b, which are related to the main vibrational modes of  $AsS_3$  and  $AsSe_3$  pyramids, respectively. With the gradual substitution of Se for S in  $As_{40}S_xSe_{60-x}$  glass system, there is a slow shift toward the higher wavenumber for the main vibrational mode (a) of  $AsS_3$ , however, there is a slight shift to the lower wavenumber for the main vibrational mode (b) of  $AsSe_3$ . This phenomenon can be explained by evolution of the nearest neighbor connection of a  $AsS_3$  ( $AsSe_3$ ) pyramid with substitution of Se for S, which is shown in Fig.3 as an example of nearest

neighbor connectivity of a central  $\text{AsS}_3$  pyramid with the increase of Se content. There are two main factors, which play important roles in the slight shift of main vibrational modes called electronic induction effect and vibrational coupling effect. When it comes to electronic induction effect, the vibrational mode frequencies are determined by vibrational force constant and reduced mass. In addition, the vibrational force constant of As-S (As-Se) bond is related to electro-negativity. As shown in Fig.3 (a), a central  $\text{AsS}_3$  pyramid is surrounded by three  $-\text{AsS}_2$  clusters. With the variation of Se/S ratio in  $\text{As}_{40}\text{S}_x\text{Se}_{60-x}$  glass, the nearest neighboring connectivity of the central  $\text{AsS}_3$  transforms from a, b, c to d in Fig.3. Firstly, in view of vibrational coupling between the central pyramid and surrounding pyramids, the slight decrease in the fraction of surrounding  $\text{AsS}_3$  pyramids instead of  $-\text{AsSe}_2$  fraction could be the cause of weakening interaction between inter-groups, because of different bond distance and energy between  $-\text{AsS}_2$  ( $-\text{AsSe}_2$ ) clusters and the central  $\text{AsS}_3$  pyramid, which lead to a gradual increase of frequency of  $\nu_1$  mode of central  $\text{AsS}_3$  pyramid in the sequence of a, b, c and d. In addition, considering the vibrational coupling of intra-central pyramid, the slight increase in the degree of distortion in symmetry, which influence the three As-S stretching vibration of the central  $\text{AsS}_3$  pyramid in the sequence of a (similar to d) and b(similar to c).the distortion of As-S bond of the central pyramid in symmetry lead to a decline of vibrational coupling of intra-central  $\text{AsS}_3$  pyramid, resulting in a slight increase of  $\nu_1$  mode of central  $\text{AsS}_3$  pyramid in the same sequence from a (similar to d) to b(similar to c).Furthermore, with a view to the variation of electro-negativity around the central pyramid induced by substitution of S by Se, the mean force constant of the central  $\text{AsS}_3$  pyramid should increase in the sequence of a, b, c and which also result in the frequency of  $\nu_1$  mode should increase in the same sequence. All these three aspects above contribute to the higher shift of  $\nu_1$  mode of  $\text{AsS}_3$  pyramid. The similar explanation can be applied to the frequency shift of  $\nu_1$  mode of  $\text{AsSe}_3$  pyramid.

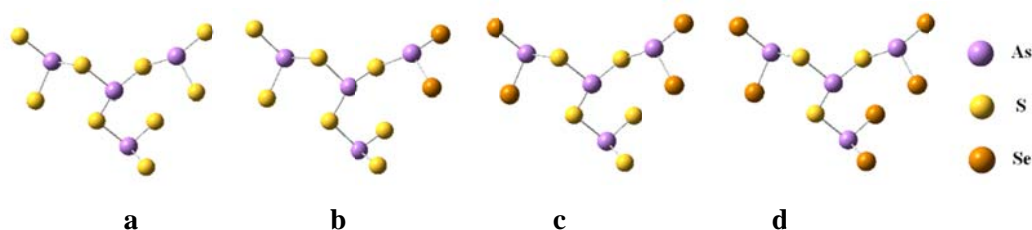


Fig.3. Schematic representation of the evolution of nearest neighbor connectivity of a central  $\text{AsS}_3$  pyramid with the increase of Se content.

## 5. Conclusion

In summary, basic vibrational modes of  $\text{AsS}_n\text{Se}_{3-n}$  pyramids were calculated by DFT, which shows the variation of point group and symmetry corresponding to the different ratios of S/Se in  $\text{AsS}_x\text{Se}_{3-x}$ . Firstly, there are similar vibrational modes between  $\text{AsCl}_3$  ( $\text{AsBr}_3$ ) and  $\text{AsS}_3$  ( $\text{AsSe}_3$ ) pyramid units, because  $V_s(\text{AsCl}_3)/V_s(\text{AsS}_3) \approx V_s(\text{AsBr}_3)/V_s(\text{AsSe}_3)$  and  $V_{as}(\text{AsCl}_3)/V_{as}(\text{AsS}_3) \approx V_{as}(\text{AsBr}_3)/V_{as}(\text{AsSe}_3)$ . In addition, the frequency variation of main vibrational modes for four basic  $\text{AsS}_x\text{Se}_{3-x}$  pyramids ( $n=0, 1, 2, 3$ ) from fast to slow can be demonstrated by force constant and reduced mass. Furthermore, Compared to the As-S related peak range of  $g\text{-As}_2\text{S}_3$ , the As-Se related peak range of  $g\text{-As}_2\text{S}_3$  shows two shoulders not like the board peak of  $g\text{-As}_2\text{S}_3$  in the  $200\sim 300\text{cm}^{-1}$ , which is because the distinction of frequency value between symmetrical ( $\nu_1$ ) and asymmetrical ( $\nu_3$ ) vibrational modes of  $\text{AsSe}_3$  pyramid is more larger than that of  $\text{AsS}_3$  pyramid. Finally, the shift of main Raman scattering frequency of structural units of  $\text{AsS}_n\text{Se}_{3-n}$  pyramids in the Raman spectroscopy of  $\text{As}_{40}\text{S}_x\text{Se}_{60-x}$  glasses can be attributed to the alteration of the nearest neighbor local surroundings with different ratios of S/Se.

This work was partially supported by NSFC (nos. 51372180, 51172169, 51032005), NSF of Hubei Province (2013CFA008), NCET (NCET-11-0687), SRFDP (20130143110013) and the key technology innovation project of Hubei Province.

## Reference

- [1] O. Kostadinova, A. Chrissanthopoulos, T. Petkova, S. N. Yannopoulos, *Journal of Solid State Chemistry* **184**, 447 (2011).
- [2] F. Y. Lin, O. Gulbitten, Z. Y. Yang, L. Calvez, P. Lucas, *Journal of Physics D-Applied Physics* **44**, 045404 (2011).
- [3] K. D. Machado, A. S. Dubiel, E. Deflon, I. M. Kostrzepa, S. F. Stolf, D. F. Sanchez, P. Jovari, *Solid State Communications* **150**, 1359 (2010).
- [4] P. Srivastava, H. S. Mund, Y. Sharma, *Physica B* **406**, 3083 (2011).
- [5] A. Pasquarello, *Current Opinion in Solid State and Materials Science* **5**, 503 (2001).
- [6] T. Uchino, T. Yoko, *Journal of Non-Crystalline Solids* **204**, 243 (1996).
- [7] K. Jackson, A. Briley, S. Grossman, *Physical Review B* **60**, 14985 (1999).
- [8] G. Lucovsky, *Physical Review B* **6**, 1480 (1972).
- [9] G. Lucovsky, R. M. Martin, *Journal of Non-Crystalline Solids* **8-10**, 185 (1972).
- [10] W. Y. Li, S. Seal, C. Rivero, C. Lopez, K. Richardson, A. Pope, A. Schulte, S. Myneni, H. Jain, K. Antoine, A. C. Miller, *Journal of Applied Physics* **98**, 053503 (2005).
- [11] M. E. Zandler, F. D. Souza, *Comptes Rendus Chimie* **9**, 960 (2006).
- [12] S. I. Simdyankin, S. R. Elliott, *Physical Review B* **69**, 144202 (2004).
- [13] M. Fabian, E. Svab, V. Pamukchieva, A. Szekeres, S. Vogel, U. Ruett, *Journal of Physics: Conference Series* **253**, 012053 (2010).
- [14] Kazuo N. *Infrared and Raman spectroscopy for inorganic and coordination compounds*, Huang Deru trans. Beijing: Chemical Industry Press, 1986.
- [15] R. M. Holomb, V. M. Mitsa, *Journal of Optoelectronics and Advanced Materials* **6**, 1177 (2004).
- [16] T. Wagner, S. O. Kasap, *Journal of Materials Science* **33**, 5581 (1998).